JOURNAL OF GEOPHYSICAL RESEARCH, VOL 95, NO D10, PAGES 16,825–16,838, SEPTEMBER 20, 1990

Daytime Turbulent Exchange Between the Amazon Forest and the Atmosphere

DAVID R. FITZJARRALD,[1] KATHLEEN E. MOORE,[1] OSVALDO M. R. CABRAL,[2] JOSÉ SCOLAR,[3,4] ANTÔNIO O MANZI,[5] AND LEONARDO D. DE ABREU SÁ[5]

Detailed observations of turbulence just above and below the crown of the Amazon rain forest during the wet season are presented. The forest canopy is shown to remove high-frequency turbulent fluctuations while passing lower frequencies. Filter characteristics of turbulent transfer into the Amazon rain forest canopy are quantified. In spite of the ubiquitous presence of clouds and frequent rain during this season, the average horizontal wind speed spectrum and the relationship between the horizontal wind speed and its standard deviation are well described by dry convective boundary layer similarity hypotheses originally found to apply in flat terrain. Diurnal changes in the sign of the vertical velocity skewness observed above and inside the canopy are shown to be plausibly explained by considering the skewness budget. Simple empirical formulas that relate observed turbulent heat fluxes to horizontal wind speed and variance are presented. Changes in the amount of turbulent coupling between the forest and the boundary layer associated with deep convective clouds are presented in three case studies. Even small raining clouds are capable of evacuating the canopy of substances normally trapped by persistent static stability near the forest floor. Recovery from these events can take more than an hour, even during midday

1 INTRODUCTION

Much of the concern in forest-atmosphere interaction to date has been in determining the heat, moisture, and momentum budgets over forests [*Hutchinson and Hicks*, 1985]. The desire among atmospheric chemists to determine natural sources and sinks of radiatively active trace gases in forests has increased interest in understanding the mechanisms of mass transport between the canopy and the atmosphere. Although transports of the trace gases are often inferred by analogy with those of heat and momentum, for example, these sources and sinks are concentrated in the upper canopy, while sources deeper in the forest may also be important to trace gases. Only a small number of observational studies of the turbulent properties of the canopy and above-canopy layers in forest environments anywhere have been published, and few of these have been conducted in the large tropical rain forests.

The structure of the Amazon rain forest is such that little (1–3%) of incident solar radiation reaches the forest floor [*Shuttleworth et al.*, 1984*b*]. Because in rain forests there is a dense canopy cover formed by the tallest trees, much of the shortwave radiation is absorbed and longwave radiation emitted to the atmosphere in the upper 20% of the canopy. Thus the heat budget during the daytime refers mainly to processes occurring near canopy top. The presence of leaves in the same layer also means that the moisture flux is concentrated there, though it is possible that momentum flux may be felt through a somewhat deeper layer. The result of radiative heating is that between forest floor and upper canopy there is nearly always a layer that is statically stable in the mean, both day and night, as illustrated in Figure 1, and this circumstance poses great difficulties for the use of simple flux-gradient models of deep-canopy exchange processes. *Denmead and Bradley* [1985] presented examples of countergradient fluxes in the Uriarra forest in Australia. Many important atmospheric constituents do not have sources and sinks coincident in the upper canopy. For example, carbon dioxide is absorbed during the daytime in the foliar upper canopy but is emitted during respiration at all levels in the forest, including emission at the forest floor that results from decay processes. Thus, for example, to understand exchange processes that accomplish the diurnal cycle of CO_2 emission [see *Fan et al.*, this issue] or nitrogen oxide emission [*Bakwin et al.*, this issue], it is necessary to consider processes that lead to coupling through the entire canopy layer.

In earlier work during the Amazon dry season [*Fitzjarrald et al.*, 1988], we studied the properties of the surface layer just above the Amazon forest canopy. In this paper we emphasize coupling between this layer and the midcanopy level, with the aim to understand mechanisms of the turbulent exchange of heat, momentum, and moisture and to relate these mechanisms to transports of trace gases into or out of the canopy. Since fluxes of the thermodynamic quantities are largest during the day and because of fundamental differences in the static stability regimes within and just above the canopy, we discuss the daytime situation in this paper, deferring the nocturnal case to a companion paper [*Fitzjarrald and Moore*, this issue]. The weak daytime stable layer near the forest top is thin, bounded below by a more stable layer and above by the convective surface layer, and fragile, being punctured at intervals by penetrating gusts we associate with cloud outflows. The nocturnal stable layer in the canopy is a downward extension of the stable boundary layer that reaches above 300 m [*Martin et al.*, 1988].

Though perfect knowledge of the bulk properties of forests (roughness and displacement lengths, transport resistances)

[1]Atmospheric Sciences Research Center, State University of New York, Albany.
[2]Centro Nacional de Pesquisa da Seringueira e Dendé—Embrapa, Manaus, Amazonas, Brazil.
[3]Departamento de Meteorologia, Universidade de São Paulo, Brazil.
[4]Now at Instituto de Pesquisas da Meteorologia, Universidade Estadual de São Paulo, Bauru, Brazil.
[5]Instituto de Pesquisas Espaciais, São José dos Campos, São Paulo, Brazil.

Paper number 89JD03438.
0148-0227/90/89JD-03438$05.00

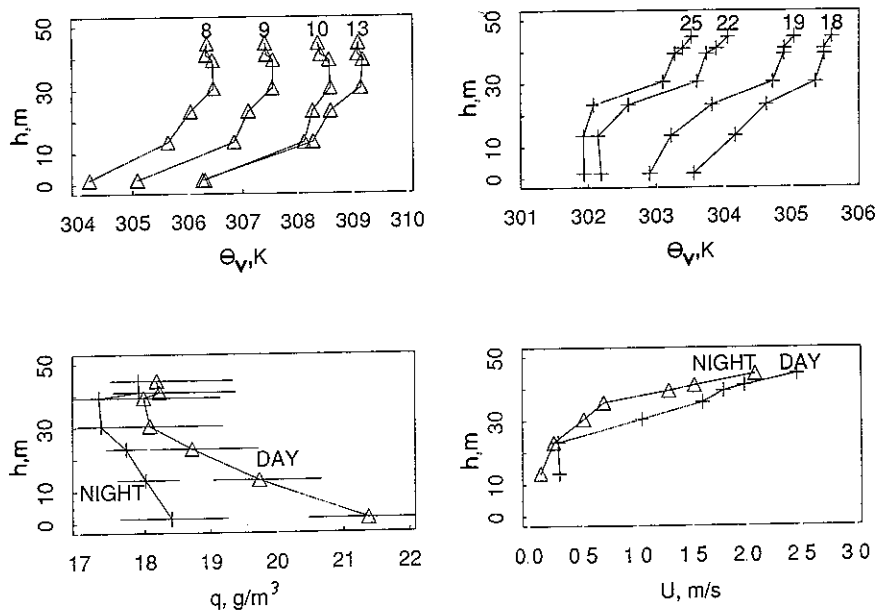

Fig. 1. Mean profiles of virtual potential temperature, Θ_v(K), specific humidity q (g m^{-3}), and wind speed U (m s^{-1}) within the canopy. The Θ_v profiles are identified by the hour of day over which they were averaged (12 = 1200; 25 = 0100)

in principle allows one to estimate the response of the forest to given forcing, it is arguably just as important to gather information on what this forcing is, especially when one is dealing with the data-sparse Amazon forest region during such a chaotic period as the wet season. The distinction between forcing and response is only a useful prototype, and one expects it to be most applicable when one considers processes such as storm outflows or convective boundary layer eddies whose scale is larger relative to that of the forest itself. At the scale of shear-dominated turbulence just above the canopy, the prototype does not work as well. Recent work [*Hunt et al.*, 1988; *Kaimal*, 1978] shows that large- and small-scale turbulence in the surface layer may be described as statistically nearly independent distributions. In this paper we aim to describe the atmospheric forcing and then consider the forest "responses," among them the fluxes at canopy top and motions within the canopy that results from the winds above.

In section 2 we present the experimental design for micrometeorological measurements in ABLE 2B and discuss the site, instrumentation, data analysis techniques, and available data. In section 3 we present (1) diurnal variation of horizontal wind fluctuations related to larger synoptic-scale variations and a comparison of horizontal wind speed spectra in raining convection over the Amazon with those seen in the dry convective boundary layer, (2) characteristic length and time scales observed in the canopy, and (3) the use of vertical velocity skewness and its budget to highlight the differences between the canopy and plane surface layers. In section 4 we focus on the vertical coupling of the layer just above the canopy and that just below the crown. Turbulent fluctuations inside the canopy are considered as filtered versions of fluctuations above. In section 5 we address the response of the forest to cloud convective downdrafts using three case studies as illustrations. The aim is to relate radar echo passage near the tower to gusts observed at canopy top. Then these gusts are related to the degree and depth of subsequent mixing into the canopy. In section 6 we identify relationships between directly measured turbulent fluxes and simpler, more readily available measurements. Conclusions and suggestions for future work are in section 7.

2 Experimental Design and Execution

Our selection and deployment of instrumentation were guided by a desire to document transient mixing episodes associated with raining convection and to study the statistical properties of the vertical coupling between the atmosphere just above the forest and the air below the canopy crown. Thus our focus included processes that occur on the order of seconds to minutes, and it was necessary to record data at more frequent intervals than in previous field campaigns. The primary observations presented here were made at the 45-m micrometeorological tower at the Ducke Forest Reserve (2°57'S, 59°57'W). *Shuttleworth et al.* [1984*a*] and *Sá et al.* [1986] present descriptions of the vegetation near the site. Trees in the region have an approximate height of 35 m, varying from 20 to 42 m, with plant density of approximately 3000 trees/ha (1 ha = 10,000 m^2) [*Shuttleworth et al.*, 1984*a*]. The dense canopy is not layered but is continuous from the 3- to 5-m-tall palms to the tallest trees at about 35 m. Occasional emergent trees reach 40 m or more in height.

Among the observations presented in this paper are those made by four automatic portable automated mesonet (PAM) stations located on 45-m towers that extended approximately 10 m above the rain forest canopy, and by the 3-cm radar operated at Eduardo Gomes Airport near Manaus, Amazonas, Brazil. Details of the PAM network location and the operating characteristics of the radar are given by *Garstang et al.* [1990]. In this paper we draw on time series of horizontal winds from the PAM stations, and constant altitude plan-position indicator (CAPPI) echo images from the radar. Profile measurements of wind speed, temperature, and humidity at the Ducke tower were made at the levels

TABLE 1 Heights and Types of Measurements Available on Ducke Tower

Height, m	INPE	SUNYA	Harvard
1.45	q, T		
2 49	q, T		
13 5	u, q, T		
23 3	u, q, T	w', T', q' (level 3)	
30 5	u, q, T		
35 7	u, q, T		
37 5	u		
39 3	u, q, T	w', T', q'	CO_2',O_3'(level2)
41 0	u, q, T		
42 8	u		
44 7	u, q, T	Gill: u', ϕ; w', T', q' (level 1)	
48 7	u, q, T		

INPE, Instituto de Pesquisas Espaciais; SUNYA, State University of New York at Albany.

indicated in Table 1, and incident solar and net radiation were observed at canopy top by the team from the Instituto de Pesquisas Espaciais (INPE). Because of some technical difficulties with the net radiation measurement during the day, we do not discuss the heat budget here. Heat balance estimates at Ducke Forest have been presented previously by *Shuttleworth et al* [1984*a*], *Sá et al.* [1986], and *Fitzjarrald et al* [1988]. The radiation and profile instruments and the data acquisition system are the same as those described by *Shuttleworth et al* [1985] with two modifications. First, to document sporadic events more completely, the slow-response profile data on the tower were acquired at 5-min instead of the previously used 20-min intervals, and wind speed sensors at 30, 25, and 13 m were replaced by Thornthwaite low-threshold cup anemometers. A summary of the instrument locations is given in Table 1.

Directly measured eddy correlation fluxes were found for 20-min averages using sets of rapid-response turbulence instruments, identical to those discussed by *Fitzjarrald et al* [1988]. These were installed at 45 m (level 1), 39 m (level 2), and 23 m (level 3) (see Table 1). Each set of instruments consisted of a Campbell Scientific vertical sonic anemometer with fine-wire thermocouple and a Campbell Scientific krypton hygrometer. Instrument response characteristics and appropriate references were given by *Fitzjarrald et al* [1988]. At the 45-m level a Gill propeller-vane anemometer was operated. Data acquisition was done using the Campbell Scientific Datalogger, to calculate and record moments, fluxes, and average quantities. The Datalogger sampled each sensor at 2-s intervals. Raw data from 13 fast channels were also recorded at 10 Hz onto the hard disk of a PDP 11/73. These data were backed up twice daily to floppy disks. The 13 signals included w, T, and q at three levels, wind speed and direction from the Gill anemometer, and two signals from the Harvard group, from their fast-response ozone and carbon dioxide instruments. Details of these instruments are presented by *Fan et al.* [this issue]. Data from the Gill anemometer were recorded by the Datalogger for 3 weeks continuously. Because the sonic anemometers were damaged by rain, there are long periods when only one of the above-canopy instruments was operating. Turbulent moment data from the PDP system were calculated by defining fluctuation to be the deviation from a centered, 5-min running mean filter operating on the raw, 10-Hz signal. Simple 20-min means were removed in the calculation of fluxes in the Dataloggers. Few large differences in 20-min averaged fluxes calculated using the PDP and the Datalogger systems were found. In spite of the difficulty of operating during the rainy season in the Amazon, a total of 138 hours of raw data were collected during the experiment.

3 CANOPY-ATMOSPHERE EXCHANGE CHARACTERISTICS DURING ABLE 2B

Horizontal Wind Speed Fluctuations

In the absence of rain in the morning, strong daytime surface heating in the Amazon typically leads to rapid convective boundary layer (CBL) growth to approximately 1300 m and subsequent cloud formation by 1100 LT [*Martin et al.*, 1988]. After noon, appreciable cloud development typically occurs; satellite images of the region show diurnal pulsing in cloud amount. During the wet season, the diurnal pattern may be enhanced or disrupted by large organized cloud systems [*Greco et al* , this issue], and the passage of these large systems punctuates a diurnal wind signal at the Ducke site. The Gill anemometer at Ducke tower and the anemometers at the four PAM stations are robust instruments. The horizontal wind record is the longest unbroken time series available in the experiment, and it is ideally suited for examining diurnal variability and characteristic length scales. Horizontal wind properties also provide a long-term reference with which to understand the shorter period of more detailed observations.

Average wind speeds during the wet season are light, with 20-min averaged wind speeds rarely exceeding 4 m/s over the 3-week period shown in Figure 2. Enhanced daytime turbulent mixing at canopy top leads to a stronger diurnal signal in σ_u than in the mean wind. It is clear that the beginning of the experiment and the last 12 days show the most pronounced diurnal signal, as noted by *Greco et al* [this issue]. Two periods with rainfall followed by very light winds and little diurnal variation (day 114 and days 120–123) were identified by Greco et al. as being dominated by large systems that propagated from the coast. *Menzel et al.* [this issue] found from satellite analysis that large cirrus shields are left in the wake of these systems, and it seems reasonable that reduced solar radiation and evaporation of rainfall from leaves could reduce how convective the above-canopy layer can be during these periods. This results in relatively long periods of time during which little turbulent exchange is likely to occur from the canopy. Although the eddy correla-

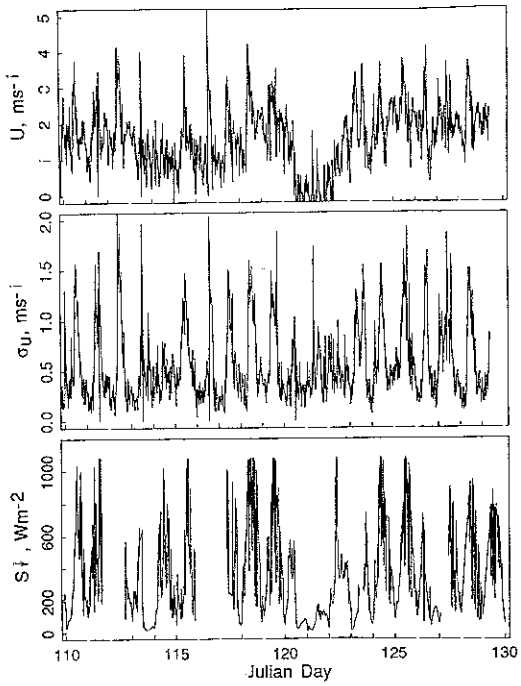

Fig 2. Time series of horizontal wind speed U (m s^{-1}) at 45 m, σ_u (m s^{-1}), and incident solar radiation S (W m^{-2}) for Julian days 110–129 (April 19 to May 9)

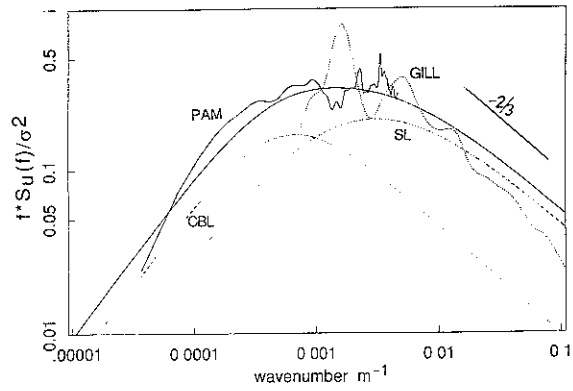

Fig. 3 Power spectrum of the horizontal wind at 45 m Solid line shows low-frequency estimate from the Ducke PAM station Dotted line shows high-frequency estimate from the Gill anemometer on the Ducke micrometeorological tower Dashed and solid curves are as indicated: convective boundary layer (CBL) and surface layer (SL) contributions to the total spectrum (solid curve), according to the curve fit by *Højstrup* [1982]

tion instrumentation operated only intermittently during the experiment, because of the many rainy periods, it is possible to estimate fluxes during these disturbed periods by inference using the σ_u data, as discussed in section 6 below

It is clear that after day 121 (May 1), diurnal changes in σ_u are more pronounced, and the solar radiation record indicates that the average onset of appreciable convective cloudiness was approximately 1100 LT The average wind speed trace (not shown) shows a drop in the afternoon The PAM stations also recorded the maximum gust in 1-min periods, but this also showed no average afternoon increase One might expect enhanced wind speed or σ_u due to the presence of convective clouds Indeed, it is at this time of day that downdrafts from raining clouds were observed to occur It appears that these events, though potentially important to total transport out of the canopy (see section 5 below), are not sufficiently frequent to influence the wind averages significantly The standard deviation in solar radiation does increase somewhat during the afternoon, reflecting the onset of convective cloudiness

Are eddies from the dry CBL contributing to the daytime maximum in σ_u presented above (Figure 2)? The spectrum of horizontal wind fluctuations in the atmospheric surface layer is broad in comparison with that of vertical velocity fluctuations *Kaimal* [1978] showed that this broadening results from the influence of large eddies on the scale of z_i, the height of the convective boundary layer *Højstrup* [1982] presented universal curve fits of spectra of horizontal wind fluctuations within and above the convective surface layer as a linear combination of a low wave number contribution from large eddies, whose size is determined by z_i, and a high wave number contribution from mechanical turbulence produced by shear near the surface This is in accordance with the concept of statistical separation of the convective and mechanical contributions to horizontal velocity variance, recently emphasized by *Hunt et al.* [1988] Over a nearly plane surface in the absence of significant cloud effects, one would therefore expect the horizontal wind speed spectrum above the forest canopy during the daytime to show the influence of CBL eddies in like manner In the equatorial trough over the Amazon rain forest during the wet season, presence of variance partition based on the dry CBL scaling laws might seem unlikely On the other hand, one observes convectively mixed layers in disturbed conditions in areas removed from the direct influence of cloud drafts in both the oceanic and continental equatorial tropics [*Martin et al.*, 1988; *Fitzjarrald and Garstang*, 1981]

An average daytime total wind speed spectrum was found using the 1-min averaged wind data from each of the PAM stations for 12 days (Figure 3) Taylor's hypothesis was used to convert from frequency to wave number, though we recognize that this may produce some distortion at the lowest wave numbers Except for transient periods near local clouds, the wind direction usually did not change significantly during the day, and we have used the total wind speed in this calculation rather than the component along the mean wind Similar spectra were obtained using the data from the other three PAM stations A typical example of the high wave number end of the spectrum, based on data from the Gill anemometer at the micrometeorological tower at Ducke for a single afternoon, shows the expected inertial subrange law above wave numbers of approximately 0.01 m^{-1}. Although the high and low wave number spectra were obtained by different instruments, for the most part they match reasonably well in the region of overlap. At lower wave numbers, we find the u spectrum to be broader than the w spectrum, a result similar to that found in the Minnesota and Kansas experiments [*Kaimal*, 1978] *Højstrup*'s [1982] model spectrum that fits the Minnesota data for typical daytime values of $z_i = 1.2$ km, $z \to 0$, $-z_i/L = 12$, is included for comparison (The result is not strongly dependent on the value of $-z_i/L$ as long as it is in the range observed during the experiment.) Because σ_u is available for the entire experiment, the spectrum here is scaled by σ_u^2 rather than by $u*^2$ An empirical relation between these quantities (see section 6 below) was used to convert the Højstrup spectrum

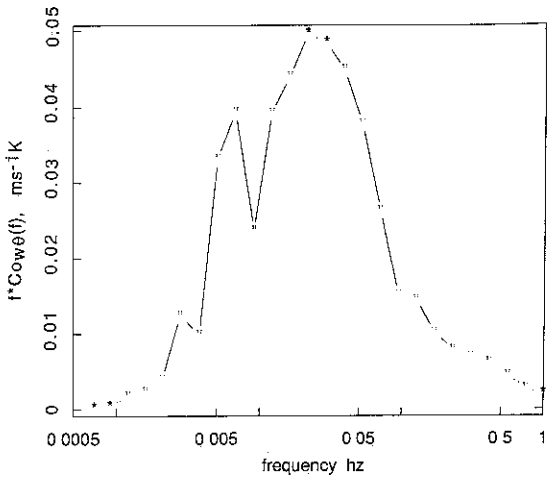

Fig 4 Mean $w\theta$ cospectrum for May 8 above the canopy (level 2 at 39 m)

to this normalization The observed average spectrum agrees remarkably well with the model spectrum, a surprising result Despite the presence of active, raining convection on many days, the average scales of motion that produce horizontal wind speed variance are the same as those seen over flat prairie during dry conditions

Characteristic Length and Time Scales

What length and time scales are characteristic of turbulence inside and just above the rain forest canopy? Within the canopy, the presence of the stable layer and vegetation makes the choice of scales difficult Inside canopy, one must question even the use of Taylor's hypothesis for obtaining length from time scales The scale of eddies that carry heat flux in the canopy layer can be deduced by reference to the average $w\theta$ cospectrum (Figure 4) to be approximately at a time scale of 30–40 s, corresponding to an approximate length scale of 100 m with the observed 3 1 m/s horizontal wind speed The time scale appropriate to the main flux-carrying eddies corresponds to an integral scale of the flux product $w\theta$ of only 3–4 s The cospectrum for wq is similar. It appears that one can "capture" the bulk of the heat and moisture fluxes and, by inference, fluxes of other substances that are emitted at similar levels in the canopy, with instrumentation with response frequencies no higher than 0 5–1 Hz.

Several candidate length and time scales observed just above and within the rain forest canopy are presented in Table 2. These include the dissipation length scale $\lambda_\varepsilon = u*^3/\kappa\varepsilon$ (κ is the von Karman constant, and ε the dissipation rate) above the canopy, the local Monin-Obukhov length L, the integral time scale of vertical velocity fluctuations at the three levels T_{wi}, and the buoyancy oscillation period $1/N$ (where N is the Brunt-Väisälä frequency) in the stable layer from 23 to 35 m, just below canopy top ($1/N_1$) and from 1 5

TABLE 2. Characteristic Length and Time Scales in and Above the Amazon Forest Canopy

Hour of Day	λ_1, m	λ_2, m	T_1, s	T_2, s	T_3, s	σ_{w1}, m s^{-1}	σ_{w2}, m s^{-1}	σ_{w3}, m s^{-1}	$1/N_1$, s	$1/N_2$, s	L, m	z_i, m
						April 29						
8–9							0.39	0 18	242	137	90	
9–10							0.63	0 27	236	122	150	
10–11		24		3 5	7 5		0.63	0 27	180	118	87	
11–12	92	27	5 3	4 9	11 2	0 45	0.62	0 32	293	102	120	
12–13	41	32	5 3	5 5	8 1	0 64	0.60	0 33	706	103	130	
13–14		38	4 8	6 0	8 4		0.52	0 26	382	94	150	
14–15		50	3 9	4 9	9 8	0 42	0.53	0 25	379	93	−34	1120
15–16	9	19	5 0	6 0	8 9	0 46	0.47	0 19	327	112	178	1200
16–17		16		8 0	14 0		0.14	0 11	167	285	285	
						May 5						
8–9		19		5 8	9 4		0 46	0.21	250	149	306	400
9–10		19		5 6	8 8		0 54	0 26	259	130	185	525
10–11		39		5 2	7 8		0 82	0 45	228	110	162	
11–12		157		4 2	7 8		0 54	0 33	226	99	157	1120
12–13		24		5 7	7 8		0 63	0 29	n/a	92	127	
13–14		17		7 5	9 3		0 46	0 22	331	97	−206	
14–15		19		7 2	9 5		0 45	0 20	n/a	118	46	
15–16		10		8 3	12 7		0 33	0 14	459	98	276	
16–17							0 32	0 14	217	115	104	
						May 8						
8–9	35	39	5 0	4 2	9 0	0 57	0 61	0 29	243	101	70	
9–10	38	21	4 2	4 2	6 8	0 71	0 74	0 33	233	92	123	560
10–11	58	25	5 0	4 5	8 0	0 63	0 65	0 35	386	90	119	800
11–12	45	23	4 5	4 5	7 5	0 68	0 69	0 36	275	97	135	
12–13	42	26	7 0	7 5	9 0	0 56	0 53	0 32	312	86	302	
13–14	20	11	8 0	6 5	13 0	0 53	0 56	0 25	186	87	−67	1200
14–15	17	0	5 0	5 0	24 0	0 21	0 24	0 13	141	132	192	
15–16							0 42	0 10	146	116	103	
16–17						0 30	0 30	0 10	197	92	−75	700

Subscripts refer to levels

to 13.5 m near the forest floor ($1/N_2$) In theory, one defines the Eulerian integral scale $T_w = \int \rho \, d\tau$, where ρ is the autocorrelation coefficient and τ is the time difference $t - t'$ between measurements; the integral extends from zero to ∞ [*Tennekes and Lumley*, 1972, p 210] Here we have followed the observational practice of *Lenschow and Stankov* [1986], defining the upper limit of this integral to be at the first zero of the autocorrelation coefficient Dissipation rates were calculated using the spectral technique, following the Kolmogoroff constants given by *Panofsky and Dutton* [1984, p 181]. We also include estimates of z_i, the convective boundary layer thickness, obtained by reference to the height of the base of the first inversion above a mixed layer in Θ_v observed in the tethered balloon profiles Some researchers have argued that the canopy height h is also an important scaling parameter to make turbulent quantities dimensionless, but we note that it is the depth to which significant turbulence penetrates that is a more suitable candidate In Figure 1, although temperature changes at all levels in the canopy during the diurnal cycle indicate that there is turbulent mixing to the forest floor, the fact that the daytime stable layer does not, on average, extend below approximately the upper third of the canopy, indicates that turbulent eddies do not typically reach below this level except during extreme events, to be discussed in section 6 Thus the relevant vertical scale for canopy turbulence might more naturally be chosen to be $h - z_d$, with z_d being a displacement height, taken here to be the mean level of momentum absorption It appears that $h - z_d$ for the Ducke Forest is approximately 15 m during the day

Panofsky and Dutton [1984, p. 176], in cautioning against the use of the integral scale in atmospheric work, noted that there has been considerable variability in reported results They cited the considerable scatter in estimates that results from using data for which trends have been inadequately removed They recommended using $T_p \sim 1/f_{\max}$, the frequency of the maximum $fS(f)$, typically 4–6 times the integral scale However, *Lenschow and Stankov* [1986] presented consistent estimates of the integral scale in the CBL, and we have followed that practical definition of T_w here D D Baldocchi and T P Meyers (A spectral and log correlation analysis of turbulence in a deciduous forest canopy, submitted to *Boundary Layer Meteorology*, 1988; hereinafter referred to as submitted manuscript) found the scale obtained from the spectral maximum to be approximately 10 times the integral scale, and we find similar results for above-canopy data However, there are additional reservations about the use of integral scales in forest canopies, which we point out in the next section

In Table 2, one sees that the integral times scales vary little with time of day or among days No significant difference exists between σ_{w1} and σ_{w2}, the vertical velocity standard deviations at the levels 1 and 2 above the canopy, and these are about twice that seen below the crown There is a difference between λ_s at the two levels above the canopy, in contrast to our earlier [*Fitzjarrald et al.*, 1988] assertion, and here it is a consequence of applying Taylor's hypothesis to change from frequency to wave number in the presence of appreciable wind shear (The w power spectra plotted against frequency at the two above-canopy levels are not appreciably different.) It is interesting to note that the buoyancy period in the stable layer ($1/N_1$ in Table 2) in the upper canopy is approximately 200–300 s, about 4 times longer than the period of the dominant flux-carrying eddies, approximately 30–40 s (Note, however, that the buoyancy period in the very stable layer near the forest floor ($1/N_2 \approx$ 100 s) is closer to that of the flux-carrying eddies) It is interesting to speculate whether or not CBL eddies might, in some circumstances, provoke sympathetic oscillations deep in the canopy during the daytime, such as we have observed at Ducke during the night [*Fitzjarrald and Moore*, this issue] It is clear that future studies should include sensitive pressure-measuring devices in the forest, as has been done by *Sigmon et al.* [1983]

Forest top is a porous boundary, and integral scales do not vary linearly with height, as they do in the plane surface layer On May 8, three levels, two above and one below the canopy top were operating, and these data demonstrate that the integral time scale of vertical velocity fluctuations does not change with height just above the canopy The autocorrelation coefficient at the three levels and their respective integrals with time lag (not shown) indicate that there is little difference between T_1 obtained at 45 m, approximately 10 m above the canopy top, and T_2, obtained at 39 m, 4 m above canopy top for this case or the additional ones listed in Table 2 However, the integral time scale T_3 at 23 m within the canopy is longer The curious result is that one finds the characteristic time scale gets longer just as one enters the canopy, and this is in agreement with what D D Baldocchi and T P Meyers (submitted manuscript, 1988) found in a Tennessee deciduous forest Table 2 indicates that our estimates for T_w in the canopy are approximately twice those seen in Tennessee An explanation for the larger T_w inside canopy is that the forest itself is only allowing eddies with longer time or length scales to penetrate These larger eddies are present in the environment above the canopy surface layer To assess this hypothesis, we must consider mechanisms of vertical exchange seen during the convective portions of the day First, we concentrate on the turbulent statistics for convective periods in relatively stationary turbulence (section 4) and then present cases of extreme events that occur during storm outflows (section 5)

Vertical Velocity Skewness

There are observed differences between the canopy and plane convective surface layers related to the vertical velocity skewness What are the differences between the daytime surface layer above the Amazon and that seen in Kansas (a classic example of a plane convective surface layer)? In the absence of nearby deep convective cloud activity in the daytime, *Martin et al* [1988] observed that a well-mixed CBL, similar to that seen over flat terrain [*Stull*, 1988], develops over the Amazon during the dry season and the same mixed layer structure was also observed during the wet season We demonstrated above that, on average, horizontal velocity spectra at canopy top behave as they do over flat terrain However, the canopy surface layer does exhibit significantly different properties from the convective plane surface layer, due in large measure to the enhanced importance of turbulent transports of eddy fluxes and variances [*Raupach and Thom*, 1981] *Raupach et al.* [1980] observed a constant flux layer in which turbulent transports were important just above a model canopy top in the wind tunnel They referred to this layer as the roughness sublayer, distinguishing it from a more conventional constant flux

layer above, in which transports are less important. In contrast to the development of observational micrometeorology in the plane surface layer, much of the work above canopies has treated the neutral case, arguably an observational anomaly over the Amazon forest and probably elsewhere, as the time series of σ_u presented earlier (Figure 2) indicates. *Fitzjarrald et al.* [1988] demonstrated that a similar roughness sublayer, with constant heat flux but appreciable buoyant and transport terms, exists over the Amazon forest, and showed that buoyancy production terms in the vertical velocity variance and heat flux budgets cannot be ignored during typical convective conditions over a forest.

Maitani [1978], showed that the vertical eddy transport of turbulent kinetic energy (TKE) is negative over a rice canopy, while the same quantity is observed to be positive in plane surface layers [*Wyngaard and Coté*, 1971]. (Note, however, that the sign of the vertical gradient of the eddy transport of TKE is positive in each instance, so that the term tends to decrease TKE in a layer near the surface.) The vertical component of this turbulent transport, $\overline{ww^2} = \overline{w^3}$, illustrates the difference between plane and canopy surface layers. Since a convectively mixed boundary layer up to approximately 1300 m is often seen above the forest canopy, there must be some level at which the boundary layer returns to its "normal" convective structure. We estimate this level by considering the properties of $\overline{w^3}$, or its normalized form, the vertical velocity skewness ($Sk_w = w^3/\sigma_w^3$). Vertical velocity skewness is typically observed to be negative above and within plant canopies in convective or neutral conditions [*Fitzjarrald et al.*, 1988; *Raupach and Thom*, 1981] and positive in convective plane surface layers [*Chiba*, 1978]. At some level above the canopy, Sk_w changes sign, and it seems reasonable to regard this level to be a measure of the beginning of the "equivalent plane surface" layer. That $Sk_w < 0$ above canopies is due largely to the fact that there is something below the "surface" in canopy layers, and there can be downward turbulent transport of vertical velocity variance associated with the drop in TKE (and σ_w^2) as one goes into the canopy. During stable conditions, the situation reverses, with $Sk_w < 0$ over the plane surface layer and, as we discuss below, >0 over the forest canopy. These diurnal differences in Sk_w may be simply understood by following reasoning recently presented by *Hunt et al.* [1988, appendix A]. Hunt et al. combined the pressure gradient and dissipation terms, assuming that they act to inhibit the growth of skewness over a relaxation time T_L. The approximate skewness budget can then be written as

$$\overline{w^3}/T_L \approx (g/\Theta_0)\overline{w^2\theta} - \alpha\overline{w^2}\partial\overline{w^2}/\partial z \qquad (1)$$

where Θ_0 is a reference potential temperature, g the acceleration of gravity, α is a proportionality constant (=1/3 for Gaussian turbulence). The constant α comes from assuming a quasi-Gaussian form for $\overline{w^2}\,\partial w^2/\partial z$. Other terms have their standard connotations. The sign of $\overline{w^3}$ (or Sk_w) is determined by the relative importance and sign of the buoyancy production term and the mechanical transport term.

Buoyancy term. The moment $\overline{w^2\theta}$ (considered as $\partial\overline{w(w\theta)}/\partial z$) is the vertical transport term in the turbulent heat flux budget equation for $\partial\overline{w\theta}/\partial t$ (considered as $\overline{w^2}(g\theta/\Theta_0)$) or as the buoyancy contribution to the $\overline{w^3}$ budget. In the convective surface layer $\overline{w^2\theta} > 0$ [*Antonia et al.*, 1982], and it is observed to be <0 in stable conditions. Over a model canopy in the wind tunnel, *Raupach et al.* [1986] found $\overline{w^2\theta} < 0$ in a narrow band near a concentrated heat source at canopy top, but it is important to note that the temperature fluctuations in this experiment were small and temperature was treated as a passive scalar. We find $\overline{w^2\theta} < 0$ during the daytime with $\overline{w^2\theta} \to 0$ at night over the Amazon forest as Ducke (Figure 5).

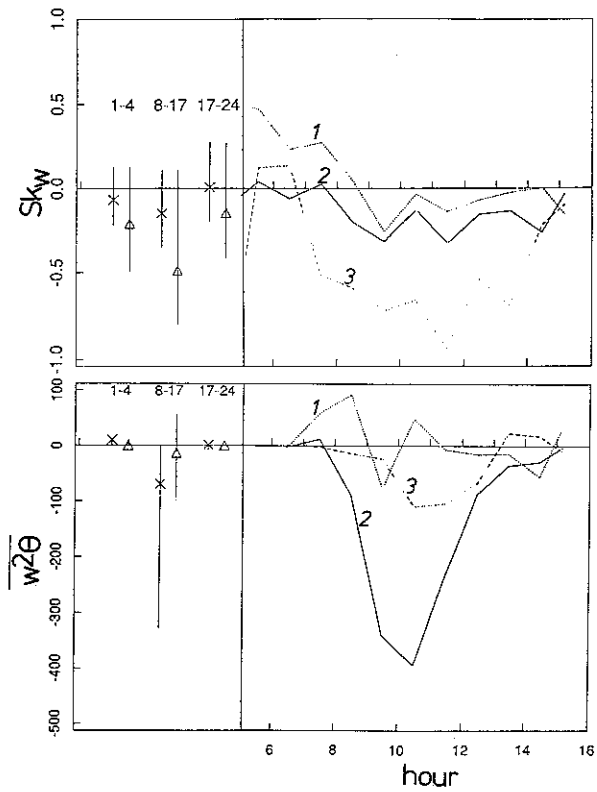

Fig. 5. (Left) The median and range of 50% of the values for several days in early morning (0100–0400), daytime (0800–1700), and evening (1700–2400) hours are plotted as additional points with vertical bars. Crosses are for level 2 (39 m), and triangles are for level 3 (23 m). (Right) Time series of Sk_w and $\overline{w^2\theta}$ during May 8.

Variance transport term. Although the mechanical transport term is only approximate, one gets insight about the sign of the contribution of this term by considering the vertical profile of $\overline{w^2}$, itself of sufficient interest to warrant some discussion. It is convenient to view $\overline{w^2}$ above the canopy as a linear combination of mechanical and convective turbulent effects [*Hunt*, 1984; *Hunt et al.*, 1988], $\overline{w^2} = au*^2 + bw*^2$, where $u*^2(= -\overline{uw})$ is the local friction velocity at a given height and $w*$ is the convective mixed layer velocity scale ($[(g/\Theta_0)\overline{w\theta}\, z_i]^{1/3}$) and a and b are empirical constants. If we assume that the CBL is well mixed in horizontal wind speed and use the mixed layer form for $\overline{w^2}(z)$ as a limiting form, the vertical profile of $\overline{w^2}$ in the lower part of the mixed layer ($z < 0.1\, z_i$) is approximately

$$\overline{w^2} = u*_0^2(1 - z/z_i) + w*^2(2z/z_i)^{2/3} \qquad (2)$$

where $u*_0$ is the friction velocity in the constant flux layer above the canopy. As expected, the shear contribution becomes less important as one leaves the surface. The level at which the two effects are equal contributors occurs at the solution of $[2w*^2/u*_0^2](z/z_i)^{2/3} + z/z_i - 1 = 0$, whose convective limit ($w*^2 \gg u*_0^2$) is approximately $z/z_i \approx 1/8$. Since

TABLE 3 Skewness Tendency Produced by Terms in the Schematic $\overline{w^3}$ Budget

	Canopy		Surface Layer	
	Day	Night	Day	Night
Buoyancy	−	≈0	+	−
Transport	−	+	−	+
Skewness (observed)	−	+	+	−

Here, $\overline{w^3}/I_L \approx [(g/\Theta_0)\ \overline{w^2\theta}] + [-\alpha\ \overline{w^2}\ \partial\overline{w^2}/\partial z]$, where the first term in brackets on the right-hand side is buoyancy and the second term in brackets is transport.

$-L$ was observed to be from 50 to 150 m on many days during ABLE 2B, $-L/z_i \approx 0.15$, and the crossover point is broadly in agreement with the $z/z_i \approx 0.1$ lower limit commonly put on the validity of convective mixed layer scaling. The importance for determining the sign of the vertical velocity skewness is that $\partial\overline{w^2}/\partial z > 0$ during CBL conditions, leading to a negative tendency for Sk_w. During the night, there is only mechanical coupling and $\partial\overline{w^2}/\partial z < 0$, this contributing a positive Sk_w tendency. A summary of the observed signs of terms in (2) for plane surface and canopy layers is shown in Table 3. In wind tunnel tests [*Raupach et al.*, 1986] and in observations over crops [*Maitani*, 1978], $\overline{w^3}$ becomes positive at 1–4 canopy heights, and we argue that this may occur at the level at which $\partial\overline{w^2}/\partial z$ changes sign. In the stable boundary layer, one expects $\partial\overline{w^2}/\partial z < 0$ just above the canopy, with $\overline{w^2}$ approaching zero at the top of the stable boundary layer [*Nieuwstadt*, 1984]. Deep in the canopy, $\partial\overline{w^2}/\partial z > 0$ at all times, and we expect, on the average, to find negative skewness there at night as well, though statistics at night may present an incomplete picture of the phenomena. We address these questions in a companion paper [*Fitzjarrald and Moore*, this issue].

The present observations support the prediction that vertical velocity skewness changes sign from day to night (Figure 5), and we can see positive Sk_w only a few meters above the canopy, in contrast to the neutral wind tunnel results. Note that Sk_w becomes more negative as one enters the canopy and that $\overline{w^2\theta}$ is most negative at level 2, approximately 4 m above canopy top (≈35 m), while it is already approaching zero at 45 m and is highly damped at 15 m below the crown. It appears that the level at which Sk_w becomes positive is not far above the canopy. During the Electra flux flight on May 4, J. Ritter (NASA Langley Research Center, personal communication, 1989) reports that $Sk_w \approx 0.6$ and $\overline{w^2\theta} \approx 0.1$ at 1.50 m. These are in the range of observations seen elsewhere in the CBL. (Hunt notes that $Sk_w \approx 0.4$ in the lower part of the typical CBL.) A linear interpolation of the skewnesses would put the Sk_w point of crossover from positive to negative at approximately 40 m above the canopy, approximately two canopy heights above the surface. Although this height is small relative to z_i, if one takes this to be the level at which one can reasonably expect to see fluxes and gradients related as they are in smoother convective plane surface layers, it is probably prohibitively high for one to consider constructing a tower in the Amazon.

4. Vertical Exchange Within the Canopy

Although vertical motions are observed within the canopy, they do not normally lead to significant heat or moisture fluxes there. For example, Θ gradients can be typically stable or near neutral in the upper canopy (Figure 1), but these conditions need not obtain for trace gas constituents. Though the sensible heat flux is small in the canopy, there appears to be a very weak downward heat flux below canopy until approximately 1000 LT, when the heat flux is upward and countergradient, in like manner to the cases presented by *Denmead and Bradley* [1985]. The average daily time series of r_{wT}, the correlation coefficient between w and T, illustrates the difference between the morning and afternoon regimes (Figure 6). As the upper canopy heats during the morning, there is downward heat flux below the crown. The bottom level shows positive heat flux only after mixing has reduced the Θ gradient, seen in the sample profiles in Figure 1 only after 1000 LT.

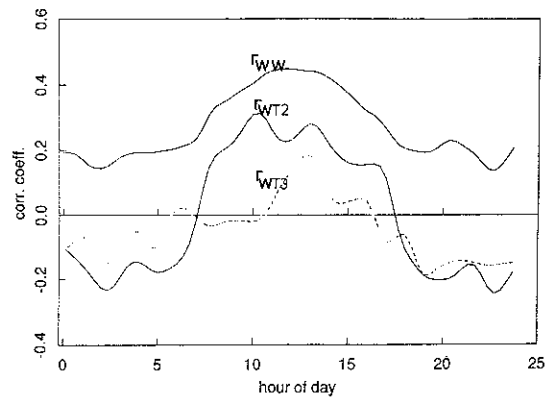

Fig. 6. Correlation coefficient r_{w2w3} between vertical velocity fluctuation above the canopy and those below the crown and r_{wT} above the canopy (solid line) and those below the crown (dashed line).

Vertical motions within the canopy reflect activity above the canopy in the daytime. The average diurnal course of the correlation coefficient between the vertical velocity above canopy and below crown at Ducke (Figure 6) shows a midday maximum near 0.45, as high a correlation coefficient as one finds between w and T or between T and q above the canopy, or indeed as high a correlation coefficient seen between turbulent variables in the plane surface layer. Vertical coupling is supressed during stable periods at night, and the correlation coefficient approaches 0.15. Time series of the correlation coefficient r_{wT} above and below the canopy (Figure 6) show that there is weak negative flux below the crown until approximately 1100 LT. At this point the in-canopy r_{wT} rises abruptly at approximately the same time that σ_u and U are decreasing, reflecting the fact that the level is turbulently coupled to the atmosphere after this time.

Inspection of typical wind signals above and below the canopy (not shown) confirms that the correlation occurs because lower frequency fluctuations are passed preferentially into the canopy. In other words, we observed the upper canopy to serve as a low-pass filter, as hypothesized in modeling work by *Wilson* [1988] and *Shaw and Seginer* [1985]. The frequency dependence of the "forest filter" effect is shown in Figure 7, a comparison of w power spectra above and below the crown and the corresponding vertical cospectrum between vertical velocities at the two levels. Frequencies above 0.03 Hz are reduced by a factor of 100, while 30% of the variance in the energy-containing range

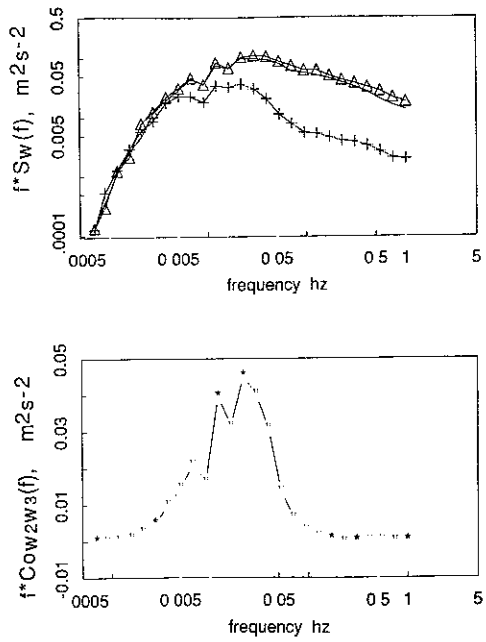

Fig. 7. Average vertical velocity power spectra for $w1$ (45 m), $w2$ (39 m), above the canopy, and $w3$ (23 m), below the crown. Also shown is the $w2 - w3$ cospectrum.

near 0.01 Hz above the canopy is passed. In contrast to *Baldocchi and Hutchison* [1988], we find the $-2/3$ inertial subrange slope of the $fS(f)$ versus f curves in logarithmic coordinates both above and within the canopy, though the onset of the inertial subrange inside the canopy occurs at a higher frequency because of the filtering effect. Filter characteristics presumably depend on the biomass density in the upper canopy. The observed median phase angle between vertical motions above and inside the canopy is small in the frequencies where most of the covariance occurs, ranging between 5° and 20°.

The fact that the vertical velocity integral scale is larger within the canopy than above (Table 2) is a simple consequence of high-frequency filtering changing spectral shapes. In theory, the integral scale is defined by the integral of the autocorrelation coefficient over all possible time lags, and the autocorrelation coefficient is the Fourier transform of the power spectrum [*Tennekes and Lumley*, 1972]. The filtering effect of the upper canopy selectively removes high-frequency variance, and this means that one should not necessarily conclude that the characteristic scale of the large eddies is different above and below the crown. It is clear from Figure 7 that a significant difference between the spectrum below the canopy and that above occurs at a particular filter cutoff frequency. If one idealizes this cutoff to be total, allowing no variance above the cutoff frequency, we find that at approximately 0.05 Hz, the integral scale for vertical velocity variance, inferred from filtering the w_2 signal, is close to that observed as the integral scale of the w_3. This result is an unavoidable consequence of combining the forest filtering effect with the definition of the integral scale and represents another way to view the action of the filter. The integral scale estimated within the canopy differs from that above in a manner determined by the forest filter cutoff frequency. One should therefore be rather cautious when ascribing comparable physical meaning to each integral scale.

5. Transient Phenomena and Transports

Atmosphere-canopy interaction during the rainy season is modulated by the effects of rain and convective clouds. Unfortunately, it is precisely during rainy periods that micrometeorological instruments often do not work properly, and indeed, one of the statistical foundations of the time series analysis of turbulent measurements, stationarity, is not really satisfied. Cloud downdrafts flood the surface layer with low-Θ_ϵ air, and as the downdraft arrives, there is usually a gust. The net effect is to reduce the static stability at all levels within the forest while temporarily increasing stability above. Although such events may be important to heat and moisture budgets, they are potentially more important to transport of substances, such as nitrogen oxides, that are produced near the forest floor and might be trapped by the persistent stable layer there [*Bakwin et al.*, this issue]. The events can be easily identified in time series plots of temperature and wind speed seen at the top of the forest. If the event happens during the middle of the day, the normal stability regime (Figure 1) returns after a time. Cloud downdraft events occur only a few times each day, and here three examples are presented. Observed response of the canopy to the downdrafts is presented and then we relate the outflows to clouds seen on the radar.

To assess the effect of cloud outflow events on turbulent fluxes, we shorten the averaging interval from the normal 20-min interval to 6.8 min, accepting the compromise that this increases the theoretical uncertainty in their values. *Wyngaard* [1983] showed that the relation among averaging time T_{ave}, required to obtain "accuracy" a, the ratio of the standard deviation of an estimate from its ensemble mean value divided by its observed mean value, in estimating the turbulent flux wx, with integral scale T_{wx} is

$$a \approx 1.4[\sigma_{wx}/\overline{wx}][T_{wx}/T_{ave}]^{0.5}$$

where σ_{wx} is the standard deviation of the sample. Observed daytime values of $T_{w\theta}$ for the heat flux product $w\theta$, for example, are typically 3 s, $\sigma_{w\theta} \approx 0.25$ m s^{-1} K, $\overline{w\theta} \approx 0.16$ m s^{-1} K and with $T_{ave} = 6.8$ min, this leads to $a \approx 0.2$. We can hope to approach within 20% of the ensemble mean during this averaging period. The value of $T_{w\theta}$ is approximately a tenth of the period of the main flux-carrying eddies seen just above the canopy, as deduced from the $w\theta$ cospectrum (Figure 4). We present some features of three cases of gusts interacting with the canopy.

Case 1, May 5, 1987. There were scattered showers on this day. Gusts from storm outflows disrupted the stability in the canopy on four marked events, approximately at 1300, at 1330, at 1417, and just after 1600. Changes in the canopy associated with the events are seen in the Θ_v and U time-height sections (Figure 8). It is apparent that only a few gusts manage to affect the canopy below 25-m altitude. The turbulent signature of one of the gusts is shown in the 1-s averaged time series above and below the canopy top (Figure 9). During the afternoon, the radar was operating, and we can clearly identify the echoes that produced the outflow gusts (Figure 10, left). It appears that the echo must pass rather close to the tower for the cloud's wake effects to

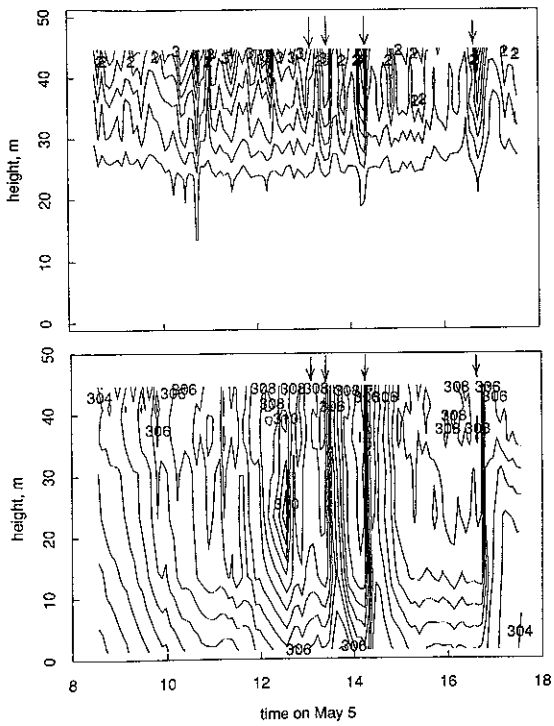

Fig. 8 Time-height section of (top) horizontal wind speed (bottom) and Θ_v on May 5. Wind speed contour interval is 0 5 m s^{-1}, Θ_v interval is 0 5 K. Cloud downdraft events referred to in the text are indicated by arrows

be felt. The cloud that produced the gust in Figure 9 passed within 2 km of the Ducke tower. Approximately neutral stability in the canopy layer appears in Figure 8 as vertical Θ_v contour lines, and the duration of the vertical contours is a measure of how long it takes the canopy to reestablish the convective canopy surface layer with its attendant stable layer below the crown. In the case of the 1330 gust, the recovery period is approximately 30 min, though in general, this time depends on how long direct solar radiation is shielded by the remnant cloud. On May 5 the gusts were produced by isolated clouds, and solar heating began just after the echo passed. Turbulent heat and moisture fluxes on this day (Figure 11) show that one effect of the clouds is to cause a peak in $w\theta$ and $\overline{wq}$, followed by a period of very small, even negative $\overline{w\theta}$, as the outflow stabilizes the canopy surface layer. The fourth event occurred just after 1600, late enough in the day that the transient stabilization from the outflow hastened the onset of the early evening stable transition. We observed this cloud to pass directly over the tower, and it brought rain. The echo was similar in size to the 1330 cloud, and the echo traveled at a similar speed. The gust was felt deep into the canopy, and the strong Θ_v inversion moved from forest floor to forest top during the event (Figure 8).

Case 2, April 29, 1987. Time-height sections for Θ_v and wind speed for this day (not shown) show that three episodes of relatively high wind speed that penetrate to the 30-m level do not result in large changes in the below-canopy thermal structure. These transient mixing episodes are weaker than during case 1. Because of signal attenuation caused by cells between the radar and Ducke, we have radar data at the tower site only after 1300. A weak cell (14 dBZ) passed over Ducke at between 1310 and 1320, and the gust penetrated only to the 30-m level in the canopy. The gust just after 1400 was apparently produced by somewhat stronger cell (27 dBZ). The main feature of the day is the squall line passage at approximately 1620. This line encompassed the entire ABLE 2B mesoscale triangle, with an echo maximum exceeding 30 dBZ passing over the tower (Figure 10, center). The effect on the canopy was pronounced, with mixing extending through the entire canopy layer. The abrupt establishment of static stability at canopy top after the line passed is similar to that observed on May 5. During the gust, vertical motions exceeding 1 0 m s^{-1} were seen above the canopy and up to 0 8 m s^{-1} within the canopy.

Case 3, May 8, 1987. Effects of cloud downdrafts were only seen during the afternoon. The time series of $\overline{w\theta}$ (Figure 12) shows relatively smooth increases up until approximately 1300. Two large outflows, at approximately 1300 and again at approximately 1400 made the forest canopy layer nearly to neutral static stability. Figure 10 (bottom) illustrates the cloud echo trajectory on May 8 around 1409 LT. From 1300 until approximately 1430, the canopy remained well mixed. Remarkable evidence demonstrating that deep canopy exchange occurred during these events is presented in Figure 12, where we include a short-section CO_2 flux observation made by the Harvard group [*Fan et al.*, this issue]. Positive sensible heat flux is coincident with negative CO_2 flux, as expected during the day when there is CO_2 uptake by the leaves. However, there is a brief period of $\overline{wCO_2} > 0$ with $\overline{w\theta} < 0$ after the second gust. It appears that the second gust, by mixing the entire canopy layer, was able to vent CO_2 accumulating during the day at the forest floor as a result of respiration into the atmosphere.

Occurrence of only a few mixing events can probably prevent accumulation of trace gases in the rain forest canopy. What is not yet clear is how to quantify what fraction of the total transport of a substance during a day can plausibly be associated with such convective mixing events. An upper limit to this transport can be estimated as follows. We consider a hypothetical trace gas s with a source at the forest

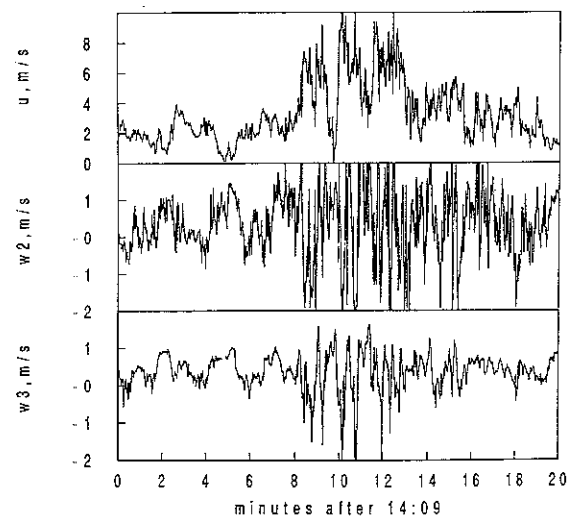

Fig. 9. An example of gust arrival at Ducke tower. (Top) Horizontal wind speed measured by the Gill anemometer (45 m). (Middle) Vertical velocity deviation from the mean at level 2 (39 m). (Bottom) Vertical deviation from the mean at level 3 (23 m).

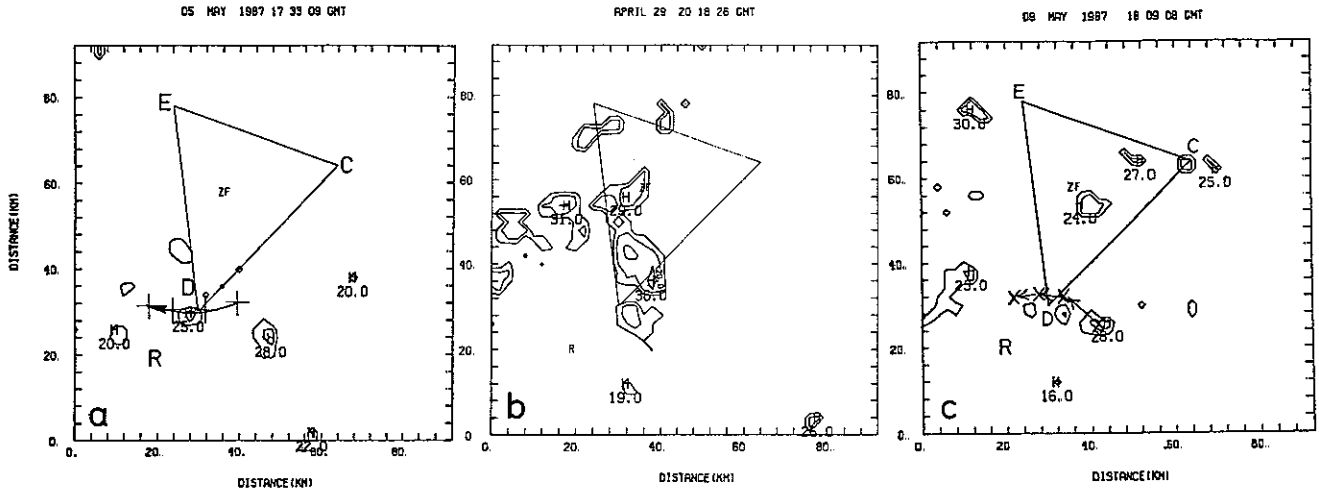

Fig. 10. (Left) Radar echo field at 1333 L T (1733 UT) on May 5. Peak echo values (dBz) are indicated. PAM station locations D (Ducke Reserve), E (Embrapa), and C (Carapanã) are shown. The center of mass of the echo near Ducke is shown at later times, indicated by the arrow trajectory. Symbols indicate cloud center of mass at 10-min intervals. (Center) Radar echo field at 1618 LT (2018 UT) on April 29 shows the squall line passing over Ducke tower. (Right) Radar echo field at 1409 LT (1809 UT) on May 8 and the cloud mass trajectory. Symbols represent location of cloud center of mass at 10-min intervals.

floor, and assume that, during a deep mixing event, a mass of the gas equal to the difference between its average canopy value $s_c = (1/H) \int s\, dz$ and its above-canopy average s_a enters the atmosphere. Noting the number of such events that occur each day, one can then augment estimates of the normal turbulent flux by the appropriate amount. The mixing events are usually sufficiently infrequent that there is time for surface emissions of a subsurface to "recharge" the canopy layer.

These examples should be sufficient to caution one from basing trace gas transport on simple analogy with heat or moisture transport. As cases 1 and 3 illustrate, even relatively small isolated raining clouds are sufficient to lead to transient periods of deep mixing and nearly neutral conditions. It is also important to observe and take into account the source and sink levels for the quantity considered. Perhaps these data may indicate first steps toward developing a model for forest-atmosphere interaction that takes into account the importance of isolated extreme events.

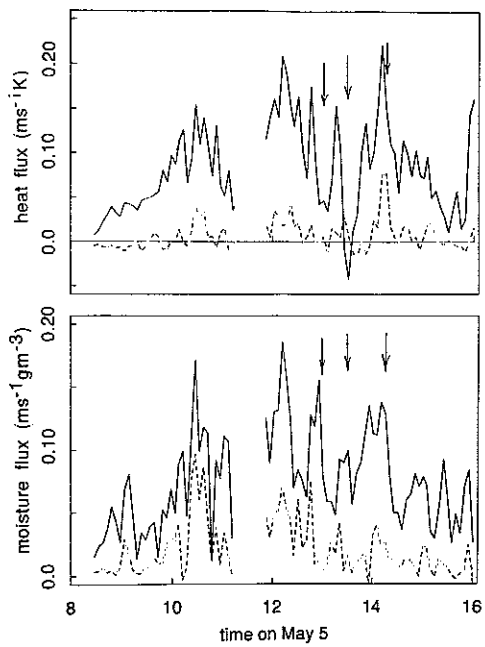

Fig. 11. Kinematic heat flux ((m s^{-1})K) and moisture ((g m^{-3})(m s^{-1})) fluxes observed during May 5. Solid line is above canopy, dashed is within canopy. Arrows indicate cloud downdraft events.

6 Empirical Relationships

To quantify horizontal gradients of flux and turbulent quantities over the Amazon, there will be a continuing need for long time series of observations at a large number of sites. However, very few towers such as that used in this work are available, and it is a continual battle to keep sophisticated instrumentation operating in the rain forest. One would like to extend the applicability of the measurements made during the short field experiment reported on here to apply to a wider area and over a longer time period. There is also continual interest among modelers in simple surface parameterizations of heat and momentum fluxes. These two interests are similar, but not identical. In the former situation, one seeks surrogate measurements, made with robust, inexpensive instruments that can operate with minimal oversight for extended periods. These measurements, such as the horizontal wind speed and its variance and solar radiation, are frequently available at climatological stations. Most large-scale models, however, do not compute variances. For such models, one seeks flux-gradient relationships to connect mean fields with the bottom boundary condition. It is clear from Figure 2 that the diurnal pulses seen most clearly in σ_u and S, but also apparent in the mean wind U, should lead to some kind of proportional relationships with sensible heat or momentum fluxes, which also vary in like manner. *Stormwind* [1987] showed that the range of static stabilities encountered during the daytime at Ducke

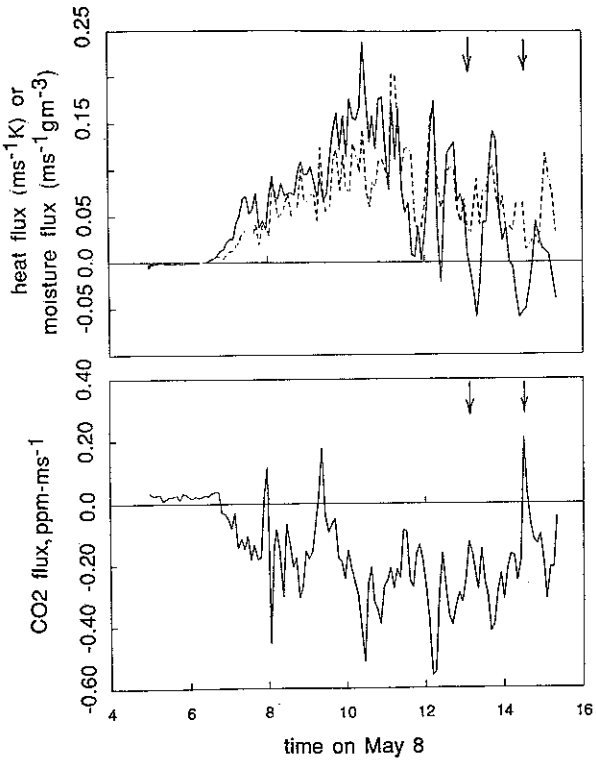

Fig 12 (Top) Kinematic heat (solid line) and moisture (dashed) fluxes observed above the canopy during May 8. (Bottom) Kinematic CO_2 flux during this period. Arrows indicate cloud downdraft events.

is very small. (He presented the histogram of $(z - d)/L$, where z is the height of the observation, d an estimate of the displacement height, and L the Obukhov length.) *Fitzjarrald et al.* [1988] showed that the drag coefficient based on the wind speed U approximately 10 m above the canopy ($C_D = u*^2/U^2$) during the middle of the day reaches an approximately constant value, 0.05, and we have found this to be true during convective periods during ABLE 2B as well ($C_D = 0.04$). Thus we anticipate finding a daytime regime for which a bulk aerodynamic flux parameterization may apply.

A major difficulty with applying such parameterizations to measurements made above forests is the uncertainty in the flux-profile relationships [*Denmead and Bradley*, 1985]. Below, we address this problem by defining the bulk flux of any quantity S to be $C_S U \Delta S$, with ΔS taken to be the difference between the value of S inside and just above the canopy. It is clear from Figure 1 and data from other similar days that the wind-induced mixing does not frequently influence the layer below 20 m, though large gradients in q, as an example, are present in the very stable layer near the forest floor. Thus we take Δq, in particular, and ΔS, in general, to be the difference between the concentration from 20- to 30-m height within the canopy and the average value above the canopy.

In the following, data for the entire experiment are averaged by hour of the day before linear regressions are calculated. Tests show reversing the order in which averaging and the linear fit is done changes the result very little. Momentum flux, as $u*^2$, is not only adequately represented by measurements of σ_u^2 ($u*^2 = 0.21\ \sigma_u^2$, $R^2 = 0.98$), but the empirical relationship follows the *Panofsky et al.* [1977] formula, corresponding to a value of $-z_i/L \approx 3$, rather smaller than the range of values observed (Table 2). However, the Panofsky et al. formula is not a strong function of z_i/L; a value of $-z_i/L = 6$ would predict a coefficient 0.16 in our regression. Our empirical relationship was used to estimate $u*^2$ from σ_u^2 to scale horizontal wind speed spectra earlier (Figure 3). A simple linear fit does a good job of predicting $H(=\rho c_p \overline{w\theta})$ from σ_u^2 (Figure 13), and σ_u is probably a good surrogate measurement for heat flux, assuming that there is sufficient solar radiation. This is because of the strongly convective nature of the midday turbulence. Although the diurnal signal in U is not as pronounced as that of σ_u, it also exhibits a reasonable linear fit with the heat flux, if one includes only periods with $\overline{w\theta} > 0$ and rejects periods with very small flux (Figure 14). Note that a linear regime, as one expects if a nearly constant product $C_H \Delta\Theta$ obtained, after 0800 is found. At Ducke, $\Delta\Theta$, as defined above, varies little during the convective portion of the day, with average values of the 39- to 45-m Θ difference being about 3 K. A linear U-$\overline{w\theta}$ relationship is consistent with the commonly used bulk aerodynamic formula $\overline{w\theta} \approx C_H U \Delta\Theta$, with C_H a transfer coefficient and U the mean horizontal wind speed. The regression line $H(\mathrm{W/m^2}) \approx 95U(\mathrm{m\ s^{-1}}) - 99$, for $U > 1$

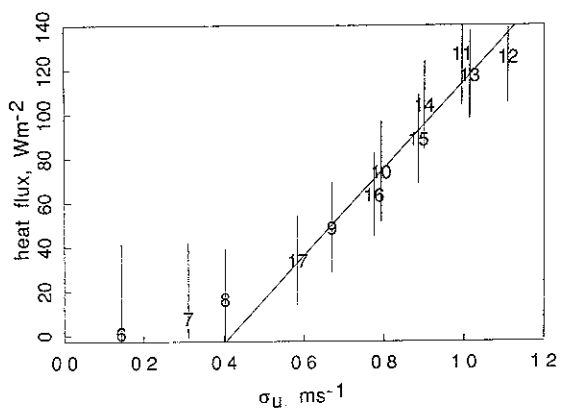

Fig 13 Relation between σ_u (m s^{-1}) and heat flux H (W m^{-2}). Points are plotted by the hour of observations. Data were averaged by hour for periods when both observations were available. The regression line is $H = -82 + 197\sigma_u$, $R^2 = 0.95$.

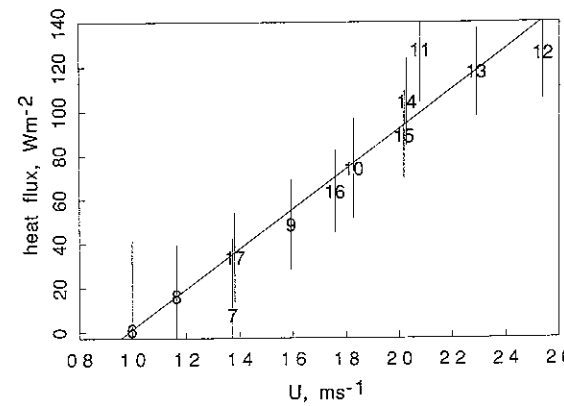

Fig 14 Relation between U (m s^{-1}), the horizontal wind speed at 45 m, and heat flux H (W m^{-2}). Data were averaged by time of day for periods when both observations were available. The regression line is $H = -89.3 + 90.6U$, $R^2 = 0.87$.

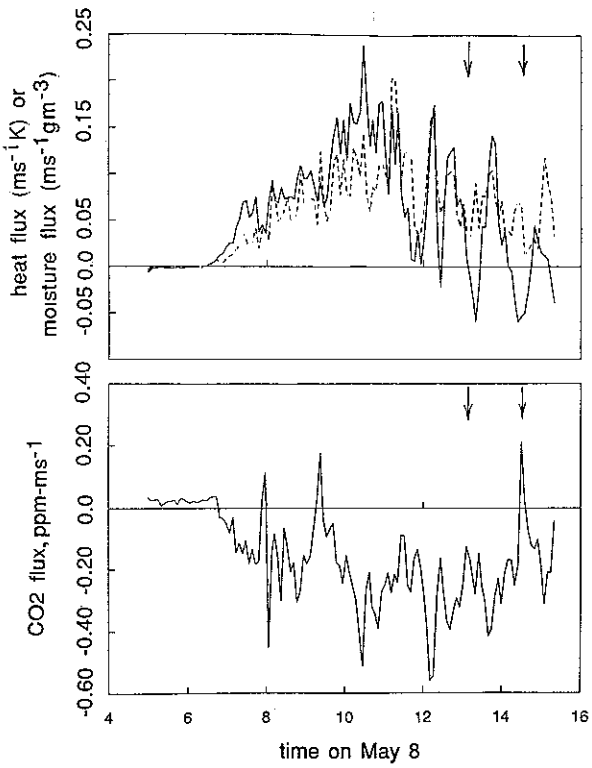

Fig 12. (Top) Kinematic heat (solid line) and moisture (dashed) fluxes observed above the canopy during May 8 (Bottom) Kinematic CO_2 flux during this period Arrows indicate cloud downdraft events

is very small. (He presented the histogram of $(z - d)/L$, where z is the height of the observation, d an estimate of the displacement height, and L the Obukhov length.) *Fitzjarrald et al* [1988] showed that the drag coefficient based on the wind speed U approximately 10 m above the canopy ($C_D = u*^2/U^2$) during the middle of the day reaches an approximately constant value, 0 05, and we have found this to be true during convective periods during ABLE 2B as well ($C_D = 0.04$). Thus we anticipate finding a daytime regime for which a bulk aerodynamic flux parameterization may apply.

A major difficulty with applying such parameterizations to measurements made above forests is the uncertainty in the flux-profile relationships [*Denmead and Bradley*, 1985]. Below, we address this problem by defining the bulk flux of any quantity S to be $C_S U \Delta S$, with ΔS taken to be the difference between the value of S inside and just above the canopy. It is clear from Figure 1 and data from other similar days that the wind-induced mixing does not frequently influence the layer below 20 m, though large gradients in q, as an example, are present in the very stable layer near the forest floor Thus we take Δq, in particular, and ΔS, in general, to be the difference between the concentration from 20- to 30-m height within the canopy and the average value above the canopy.

In the following, data for the entire experiment are averaged by hour of the day before linear regressions are calculated. Tests show reversing the order in which averaging and the linear fit is done changes the result very little. Momentum flux, as $u*^2$, is not only adequately represented by measurements of σ_u^2 ($u*^2 = 0.21\ \sigma_u^2$, $R^2 = 0\ 98$), but the empirical relationship follows the *Panofsky et al.* [1977] formula, corresponding to a value of $-z_i/L \approx 3$, rather smaller than the range of values observed (Table 2). However, the Panofsky et al formula is not a strong function of z_i/L; a value of $-z_i/L = 6$ would predict a coefficient 0.16 in our regression Our empirical relationship was used to estimate $u*^2$ from σ_u^2 to scale horizontal wind speed spectra earlier (Figure 3). A simple linear fit does a good job of predicting $H(=\rho c_p \overline{w\theta})$ from σ_u^2 (Figure 13), and σ_u is probably a good surrogate measurement for heat flux, assuming that there is sufficient solar radiation This is because of the strongly convective nature of the midday turbulence Although the diurnal signal in U is not as pronounced as that of σ_u, it also exhibits a reasonable linear fit with the heat flux, if one includes only periods with $\overline{w\theta} > 0$ and rejects periods with very small flux (Figure 14) Note that a linear regime, as one expects if a nearly constant product $C_H \Delta\Theta$ obtained, after 0800 is found At Ducke, $\Delta\Theta$, as defined above, varies little during the convective portion of the day, with average values of the 39- to 45-m Θ difference being about 3 K. A linear U-$\overline{w\theta}$ relationship is consistent with the commonly used bulk aerodynamic formula $\overline{w\theta} \approx C_H U \Delta\Theta$, with C_H a transfer coefficient and U the mean horizontal wind speed. The regression line $H(\mathrm{W/m^2}) \approx 95U(\mathrm{m\ s^{-1}}) - 99$, for $U > 1$

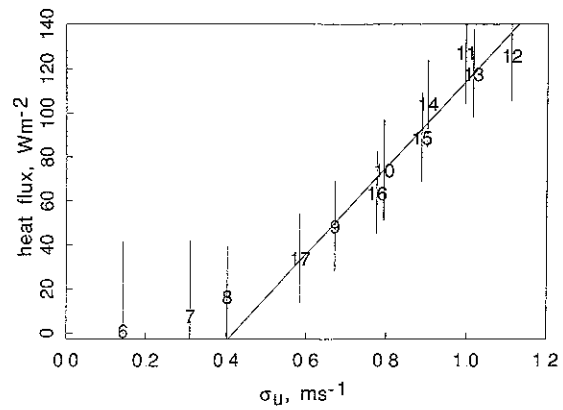

Fig 13 Relation between σ_u (m s^{-1}) and heat flux H (W m^{-2}). Points are plotted by the hour of observations Data were averaged by hour for periods when both observations were available The regression line is $H = -82 + 197\sigma_u$, $R^2 = 0.95$

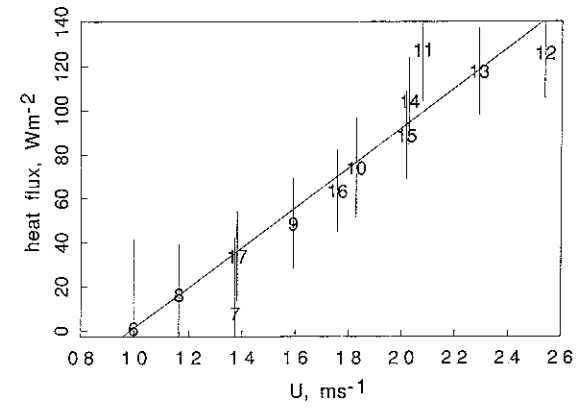

Fig. 14. Relation between U (m s^{-1}), the horizontal wind speed at 45 m, and heat flux H (W m^{-2}). Data were averaged by time of day for periods when both observations were available. The regression line is $H = -89\ 3 + 90.6U$, $R^2 = 0.87$.

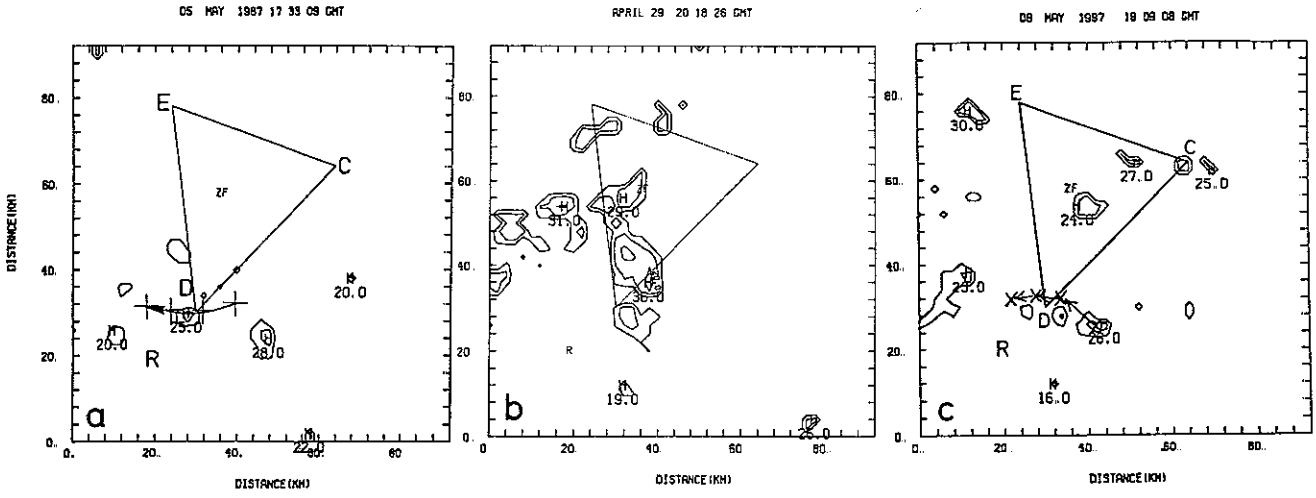

Fig. 10. (Left) Radar echo field at 1333 LT (1733 UT) on May 5. Peak echo values (dBz) are indicated. PAM station locations D (Ducke Reserve), E (Embrapa), and C (Carapanã) are shown. The center of mass of the echo near Ducke is shown at later times, indicated by the arrow trajectory. Symbols indicate cloud center of mass at 10-min intervals. (Center) Radar echo field at 1618 LT (2018 UT) on April 29 shows the squall line passing over Ducke tower. (Right) Radar echo field at 1409 LT (1809 UT) on May 8 and the cloud mass trajectory. Symbols represent location of cloud center of mass at 10-min intervals.

floor, and assume that, during a deep mixing event, a mass of the gas equal to the difference between its average canopy value $s_c = (1/H) \int s\, dz$ and its above-canopy average s_a enters the atmosphere. Noting the number of such events that occur each day, one can then augment estimates of the normal turbulent flux by the appropriate amount. The mixing events are usually sufficiently infrequent that there is time for surface emissions of a subsurface to "recharge" the canopy layer.

These examples should be sufficient to caution one from basing trace gas transport on simple analogy with heat or moisture transport. As cases 1 and 3 illustrate, even relatively small isolated raining clouds are sufficient to lead to transient periods of deep mixing and nearly neutral conditions. It is also important to observe and take into account the source and sink levels for the quantity considered. Perhaps these data may indicate first steps toward developing a model for forest-atmosphere interaction that takes into account the importance of isolated extreme events.

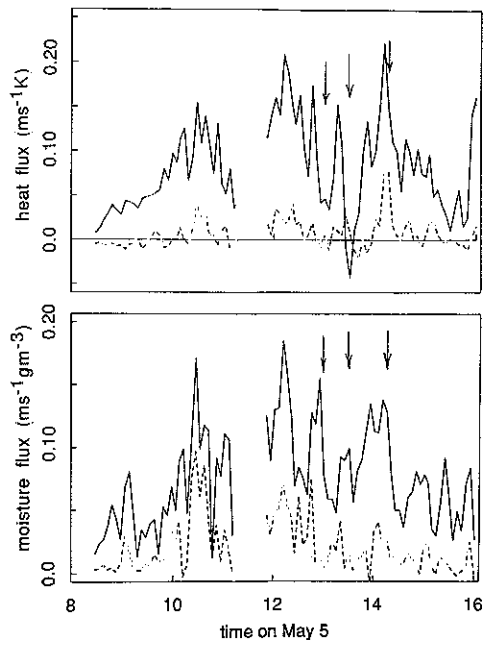

Fig. 11. Kinematic heat flux ((m s^{-1})K) and moisture ((g m^{-3})(m s^{-1})) fluxes observed during May 5. Solid line is above canopy, dashed is within canopy. Arrows indicate cloud downdraft events.

6. Empirical Relationships

To quantify horizontal gradients of flux and turbulent quantities over the Amazon, there will be a continuing need for long time series of observations at a large number of sites. However, very few towers such as that used in this work are available, and it is a continual battle to keep sophisticated instrumentation operating in the rain forest. One would like to extend the applicability of the measurements made during the short field experiment reported on here to apply to a wider area and over a longer time period. There is also continual interest among modelers in simple surface parameterizations of heat and momentum fluxes. These two interests are similar, but not identical. In the former situation, one seeks surrogate measurements, made with robust, inexpensive instruments that can operate with minimal oversight for extended periods. These measurements, such as the horizontal wind speed and its variance and solar radiation, are frequently available at climatological stations. Most large-scale models, however, do not compute variances. For such models, one seeks flux-gradient relationships to connect mean fields with the bottom boundary condition. It is clear from Figure 2 that the diurnal pulses seen most clearly in σ_u and S, but also apparent in the mean wind U, should lead to some kind of proportional relationships with sensible heat or momentum fluxes, which also vary in like manner. *Stormwind* [1987] showed that the range of static stabilities encountered during the daytime at Ducke

m s^{-1}, with a temperature difference of 3 K leads to an estimate of $C_H \approx 0.03$, a commonly observed value over rough surfaces [*Stull*, 1988], though in normal usage, one does not include an offset term. A similar regression line was found for the latent heat flux ($LE = L\overline{wq}$): LE (W/m^2) = $207U - 244$. The average daytime value of the bulk transfer coefficient for q is $C_q = 0.07$, similar to the drag coefficient. Another popular method of estimating trace gas fluxes is to use a deposition (or "emission") velocity, defined as $\overline{wq}/\Delta q$ ($=C_q U$, in terms of the bulk formulas). We find the emission to be approximately 0.15 m s^{-1} during the middle of the day, and its near constancy probably reflects the small range of wind speeds seen in the Amazon. A linear relationship between incoming solar radiation and σ_u^2, similar to that between $u*^2$ and σ_u^2 was also found, reflecting the average diurnal behavior of these quantities. We tested other empirical forms, among them the proposed relationship between temperature skewness and $\overline{w\theta}$ of *Tillman* [1972], but no clear relationships were found.

We do not suggest that the formulas presented here have universal validity, but they may be extremely useful when applied to extending the limited measurements available for the Amazon rain forest. They contain implicitly the physical correlations between elements of the heat balance at canopy top and the control that static stability exerts on turbulent fluxes, and the net effect of dry and moist convective motions on the boundary layer. One should use the bulk transport to estimate trace gas fluxes judiciously, bearing in mind the importance of individual events to effect large transient transports sporadically (section 5).

7 Conclusions and Recommendations

Conclusions

1. Filter characteristics of turbulent transfer into the Amazon rain forest canopy have been quantified, and it is clear the eddies on the scale of 50–200 m are important below the crown as well as just above the canopy.

2. Convective processes during the rainy season can alter the diurnal course of turbulent fluxes. In wake of giant coastal systems, no significant wind speed variations, and by inference, no significant heat or moisture fluxes can occur for up to a day after the event.

3. The frequency distribution of horizontal wind speed variance, on average, is well described by dry CBL similarity hypotheses, in spite of ubiquitous presence of clouds during the rainy season. The turbulent environment of the upper canopy is strongly linked to processes occurring in the entire CBL. One cannot describe the daytime canopy-atmosphere interaction completely without reference to the prevailing boundary layer state.

4. Observed large increases in the integral scale for vertical velocity fluctuations inside the canopy in comparison to that above the canopy can be understood as another aspect of the filtering effect of foliage in the upper canopy on the turbulent fluctuations, a process in which high-frequency turbulence is selectively produced and dissipated there.

5. Diurnal changes in the sign of the vertical velocity skewness observed above and inside the canopy can plausibly be explained by elements of the skewness budget, and the buoyant production term appears to play an important role.

6. Even small raining clouds can evacuate the canopy of accumulated trace gases. Recovery can take up to 1 hour, even during midday, but if storm passage occurs late in the day, a period of canopy layer static stability caused by the outflow persists into the evening transition, producing an effective "early nightfall." Deep mixing events in the Amazon appear always to be related to storm outflows. Although these events are infrequent (one to four times per day), they are potentially capable of removing gases that accumulate at the forest floor.

7. To understand details of turbulent processes in the Amazon forest canopy, it is absolutely necessary to consider the fact that the canopy is stably stratified in the mean. On undisturbed days, repeatable sequences of environments occur, and perhaps it is more instructive to look at temporal sequences of structure, to understand processes, than to categorize turbulent fluxes using stability indices.

8. Simple empirical relations for surrogate flux measurements open the possibility of operating larger networks of surface sites for long periods of time in the Amazon. Standard deviation of the horizontal wind, when averaged over long periods of time, correlates well with turbulent sensible and latent heat fluxes. Estimates of mean exchange velocities for substances whose gradients are known in the upper canopy and just above permit rough estimates of fluxes of these quantities. However, case studies show that, if a substance accumulates at the forest floor, this parameterization may be mechanistically flawed.

Recommendations

Larger networks of surface stations are needed if regional differences in heat and moisture fluxes are to be monitored in the Amazon rain forest. In particular, growing concern over deforestation and subsequent regrowth emphasizes the importance of quantifying the physical and chemical differences that are already occurring as the surface changes. It remains the case that the only detailed micrometeorological experiments in the Brazilian Amazon have come from the tower at Ducke.

More generally, the results presented here suggest to us that expanding the concept of the "forest filter" to include quantitatively the relation between the biomass density profile and the filter transfer function would be a fruitful area of continuing research. There is a need to relate vertical velocity skewness values and gradients to the height at which the forest appears to the atmosphere above as identical to the familiar plane convective surface layer. This may be an area in which careful modeling efforts would be useful. The difficulties we found in relating the integral scales to the scales of the predominant eddies just above the canopy point out the limitations of traditional spectral analysis. Recently, *Mahrt* [1989] presented idealized time series to illustrate his contention that, in prototypically convective conditions, edges between larger structures can contribute to high-frequency variance in a manner that has little to do with the traditional inertial subrange energy cascade. In future work, it would be prudent to consider Mahrt's suggestions on the use of different structure functions in place of exclusive reliance on spectra.

Acknowledgments. This work, part of the GTE/ABLE 2B field mission, was supported by NASA grant NAG-1-692 to the Atmospheric Sciences Research Center (ASRC) at the State University of New York at Albany and by INPE, the Brazilian Space Institute.

G G Lala of ASRC helped with experiment planning and wrote the Datalogger acquisition program in the field Amauri P de Oliveira assisted with operations in the field and offered advice at ASRC We are grateful to J W Sicker at ASRC for technical support before and after the experiment In Manaus, researchers from the Instituto Nacional de Pesquisas da Amazônia (INPA) and from INPE were very helpful Special thanks go to S Wofsy, P Bakwin, and S.-M Fan, all of Harvard University, who went to extra trouble to help record the large amounts of raw data obtained during this experiment. M Garstang, C Martin, S. Greco, and colleagues at the University of Virginia and at Simpson Weather Associates operated the radar and PAM systems in the field and graciously provided access to radar and PAM data sets Operating our instruments and acquiring the data presented in this paper depended in large part on the cheerful cooperation of other research teams from both Brazil and the United States that were in the field during ABLE 2B Useful comments from anonymous reviewers helped to improve the manuscript.

REFERENCES

Antonia, R A., A J Chambers, and E F Bradley, Third- and fourth-order mixed moments of turbulent velocity and temperature fluctuations in the atmospheric surface layer, *Boundary Layer Meteorol*, *22*, 421–430, 1982

Bakwin, P S , S C Wofsy, S.-M Fan, M Keller, S Trumbore, and J Maria da Costa, Emission of nitric oxide (NO) from tropical forest soils and exchange of NO between the forest canopy and atmospheric boundary layers, *J. Geophys Res* , this issue.

Baldocchi, D D., and B A Hutchinson, Turbulence in an almond orchard: Spatial variations in spectra and coherence, *Boundary Layer Meteorol* , *42*, 293–311, 1988.

Chiba, O , Stability dependence of the vertical velocity skewness in the atmospheric surface layer, *J Meteorol Soc Jpn* , *56*, 140–142, 1978.

Denmead, O T , and E F Bradley, Flux-gradient relationships in a forest canopy, in *The Forest-Atmosphere Interaction*, edited by B H Hutchinson and B B Hicks, pp 421–442, D Reidel, Hingham, Mass , 1985

Fan, S -M., S C Wofsy, P S Bakwin, and D J Jacob, Atmosphere-biosphere exchange of CO_2 and O_3 in the central Amazon forest, *J Geophys Res.*, this issue

Fitzjarrald, D R , and M. Garstang Vertical structure of the tropical boundary layer, *Mon Weather Rev* , *109*, 1512–1526, 1981

Fitzjarrald, D R , and K E Moore, Mechanisms of nocturnal exchange between the rain forest and the atmosphere, *J Geophys Res* , this issue

Fitzjarrald, D R , B L Stormwind, G Fisch, and O M R Cabral, Turbulent transport observed just above the Amazon forest, *J Geophys. Res* , *93*, 1551–1563, 1988.

Garstang, M., et al , The Amazon Boundary Layer Experiment (ABLE 2B): A meteorological perspective, *Bull Am Meteorol Soc* , *71*, 19–32, 1990

Greco, S , R Swap, M. Garstang, S Ulanski, M Shipham, R C Harriss, R Talbot, M O Andreae, and P Artaxo, Rainfall and surface kinematic conditions over central Amazonia during ABLE 2B, *J. Geophys Res* , this issue

Højstrup, J , Velocity spectra in the unstable planetary boundary layer, *J. Atmos. Sci* , *39*, 2239–2249, 1982

Hunt, J C R , Turbulence structure in thermal convection and shear-free boundary layers, *J Fluid Mech* , *138*, 161–184, 1984

Hunt, J C R , J C Kaimal, and J E Gaynor, Eddy structure in the convective boundary layer—New measurements and new concepts, *Q J R Meteorol. Soc* , *114*(482), 827–858, 1988.

Hutchison, B. A., and B B Hicks, *The Forest-Atmosphere Interaction*, D. Reidel, Hingham, Mass , 1985

Kaimal, J C., Horizontal velocity spectra in an unstable surface layer, *J. Atmos Sci* , *35*, 18–24, 1978

Lenschow, D H., and B B Stankov, Length scales in the convective boundary layer, *J. Atmos Sci* , *43*, 1198–1209, 1986

Mahrt, L., Intermittency of atmospheric turbulence, *J Atmos Sci.*, *46*, 79–95, 1989

Maitani, T , On the downward transport of turbulent kinetic energy in the surface layer over plant canopies, *Boundary Layer Meteorol.*, *14*, 571–584, 1978

Martin, C. L , D Fitzjarrald, M. Garstang, A P Oliveira, S Greco, and E Browell, Structure and growth of the mixing layer over the Amazonian rain forest, *J Geophys Res* , *93*, 1361–1375, 1988

Menzel, W P , T. J Schmit, and D P Wylie, Cloud characteristics over central Amazonia during GTE/ABLE 2B derived from multispectral visible and infrared spin scan radiometer atmospheric sounder (VAS) observations, *J. Geophys Res.*, this issue

Nieuwstadt, F T M , The turbulent structure of the stable, nocturnal boundary layer, *J Atmos. Sci* , *41*, 2202–2216, 1984

Panofsky, H A., and J. A Dutton, *Atmospheric Turbulence*, John Wiley, New York, 1984

Panofsky, H A , H Tennekes, D H. Lenschow, and J C Wyngaard, The characteristics of turbulent velocity components in the surface layer under convective conditions, *Boundary Layer Meteorol.*, *11*, 355–361, 1977

Raupach, M R , A Lagrangian analysis of scalar transfer in vegetation canopies, *Q J R. Meteorol. Soc.*, *113* 107–120, 1987

Raupach, M R , and A S Thom, Turbulence in and above plant canopies, *Annu. Rev. Fluid Mech* , *13*, 97–129, 1981.

Raupach, M R , A S Thom, and I Edwards, A wind-tunnel study of turbulent flow close to regularly arrayed rough surfaces, *Boundary Layer Meteorol* , *18*, 373–397, 1980

Raupach, M R., P A Coppin, and B J Legg, Experiments on scalar dispersion within a model plant canopy, I, The turbulence structure, *Boundary Layer Meteorol.*, *35*, 21–52, 1986

Sá, L D A , Y Viswandadham, and A O Manzi, Energy receipt partitioning over the Amazon forest, *Publ INPE-3980-PRE/990*, Inst de Pesquisas Espaciais, São José dos Campos, São Paulo, Brazil, 1986

Shaw, R H , and I Seginer, The dissipation of turbulence in plant canopies, in *7th Symposium on Turbulence and Diffusion*, pp 200–203, American Meteorological Society, Boston, Mass , 1985.

Shuttleworth, W J , et al , Eddy correlation measurements of energy partition for Amazonian forest, *Q J R Meteorol Soc* , *110*, 1143–1162, 1984*a*

Shuttleworth, W J , et al., Observations of radiation exchange above and below Amazonian forest, *Q J R Meterol Soc* , *110*, 1163–1169, 1984*b*

Shuttleworth, W J., et al , Daily variations of temperature and humidity within and above Amazonian forest, *Weather*, *40*(4), 102–108, 1985.

Sigmon, J T , K R Knoerr, and E J Shaughnessy, Microscale pressure fluctuations in a mature deciduous forest, *Boundary Layer Meteorol.*, *27*, 345–358, 1983.

Stormwind, B L., Turbulent transport above the Amazon forest, M.S. thesis, Dep of Atmos Sci , State Univ of New York, Albany, 1987

Stull, R. B , *An Introduction to Boundary Layer Meteorology*, 666 pp , Kluwer Academic, Boston, 1988

Tennekes, H., and J. L Lumley, *A First Course in Turbulence*, 300 pp., MIT Press, Cambridge, Mass , 1972

Tillman, J E., The indirect determination of stability, heat and momentum fluxes in the atmospheric boundary layer from simple scalar variables during dry unstable conditions, *J Appl Meteorol* , *11*, 783–792, 1972.

Wilson, J D , A second-order closure model for flow through vegetation, *Boundary Layer Meteorol* , *42*, 371–392, 1988

Wyngaard, J C , Lectures on the planetary boundary layer, in *Mesoscale Meteorology—Theories, Observations and Models*, edited by D. K Lilly and T Gal-Chen, pp 603–650, D Reidel, Hingham, Mass , 1983

Wyngaard, J C., and O R Coté, The budgets of turbulent kinetic energy and temperature variance in the atmospheric surface layer, *J Atmos Sci* , *28*, 190–201, 1971.

O M R Cabral, Centro Nacional de Pesquisa da Seringueira e Dendé—Embrapa, Manaus Amazonas, Brazil.

D R Fitzjarrald and K E Moore, Atmospheric Sciences Research Center, 100 Fuller Road, State University of New York, Albany, NY 12205.

A O Manzi and L D A Sá, Insituto de Pesquisas Espaciais, São José dos Campos, São Paulo Brazil.

J Scolar, Instituto de Pesquisas da Meteorologia, Universidade Estadual de São Paulo Bauru, São Paulo, Brazil.

(Received May 19, 1989;
revised August 8, 1989;
accepted November 3, 1989.)